Original Article

Institution of MECHANICAL ENGINEERS

Journal of RAIL AND RAPID TRANSIT

Proc IMechE Part F:
J Rail and Rapid Transit
2015, Vol. 229(1) 48–57

DOI: 10.1177/0954409713497199
pif.sagepub.com

SAGE

Twin-tube- and bypass-containing magneto-rheological damper for use in railway vehicles

Chaoyang Guo, Xinglong Gong, Luhang Zong, Chao Peng and Shouhu Xuan

Abstract

A 9-kN magneto-rheological (MR) damper for lateral suspension control of a railway vehicle is created in this paper. The twin-tube style is adopted in order to obtain a long damper stroke and guarantee the symmetry of the output damping force. A bypass MR valve with a radial flow path is utilised to control the generated damping force. Three-dimensional finite element analysis studies are performed to determine the magnetic field strength inside the MR valve region. The MR damper is mathematically modelled for the situation of a unidirectional fluid flow in the chamber and valve. The test results indicate that the MR damper can produce a considerable range of dynamic force and can operate as a fail-safe device. Sedimentation is detected in the damper; however, the response time is acceptable for real-world deployment.

Keywords

Magneto-rheological fluid, magneto-rheological damper, twin-tube, bypass, radial flow, railway vehicle

Date received: 29 November 2012; accepted: 18 June 2013

Introduction

Magneto-rheological (MR) fluids are a class of smart materials created by the suspension in a carrier fluid of micron-sized particles that can be magnetised. Their rheological properties can be quickly changed in a reversible manner using an external magnetic field.[1] MR fluids are used in many industrial areas and are being increasingly considered for various applications in automotive manufacturing,[2] biomedical equipment,[3] large-scale seismic control devices,[4,5] and in the polishing industry.[6] A promising device, the MR damper, can offer the advantages of a large range of damping force, highly reliable operation and good robustness with a reliable fail-safe performance while consuming very little energy. Therefore, MR dampers have received significant attention for application in semi-active control systems.[7–9]

High-speed railways have been developed by many countries since they are an efficient and economic means of transportation. However, increasing a train's speed can degrade the ride quality since significant vibrations are generated.[10] Recently, MR-based semi-active double-ended control dampers have been employed to ensure ride comfort and safety of trains. Governing equations to model a railway vehicle with multiple degrees of freedom (generally, 17 degrees of freedom) and with integrated MR dampers have been developed, and the motion of a carbody simulated.[11–14] The obtained results indicate that a semi-active controlled MR damper-based suspension system is effective for use in railway vehicles. The carbody acceleration is significantly reduced, and the acceleration of the trucks and wheelsets can be increased to some extent. Atray and Roschke[15,16] presented the design, fabrication, testing and modelling of an MR damper for the vibration control of a 70-ton railcar. A neuro-fuzzy technique was developed for a two-degree-of-freedom quarter-car model of the railcar. Two parallel MR dampers were simulated, and the results indicate that semi-actively controlled MR dampers can reduce vibration to acceptable levels if sufficient force is supplied by the dampers.

It has been suggested in the literature that MR dampers are a good choice to create good ride comfort and safety in high-speed railway vehicles. Three different control strategies have been proposed (i.e. skyhook, dynamic compensation, and dynamic compensation with acceleration feedback) to control

Department of Modern Mechanics, University of Science and Technology of China, People's Republic of China

Corresponding author:
Xinglong Gong, Department of Modern Mechanics, CAS Key Laboratory of Mechanical Behavior and Design of Materials, University of Science and Technology of China, Hefei 230027, People's Republic of China.
Email: gongxl@ustc.edu.cn

a MR damper and reduce vibrations in high-speed railway vehicles.[17–19] The dynamic compensation with acceleration feedback strategy has outperformed the other approaches in all performed tests and proved suitable for application on high-speed railway vehicles. [17–19] Recently, Gao and Yang[20] and Hudha et al.[21] pointed out that an MR damper can be used for semi-active vibration control of the suspension systems of railway vehicles. However, full-scale vehicle tests with semi-active MR dampers have not been performed to date due to the complexity of the experimental tests. Although several MR damper prototypes have been designed, practical MR dampers for railway vehicles are still rare.[11,15,21]

In this paper, a practical MR damper for railway vehicles is designed, fabricated and tested. The twin-tube style and a bypass MR valve with radial flow path are adopted for the damper. These choices extend the stroke of the damper and make the manufacturing process simpler. The unique single-flow direction improves the anti-sedimentation property of the MR fluid in the damper. The magnetic field strength is calculated by three-dimensional finite element modelling. A theoretical model is proposed to calculate the damping force. Evaluation of the MR damper indicates that the proposed damper can meet the requirements for application in railway vehicles.

MR damper

MR damper design

MR dampers can be divided into three common categories: mono-tube; double-ended; and twin-tube.[22] Mono-tube dampers have only one reservoir and an accumulator to accommodate the volume change resulting from movement of the piston rod; it is commonly applied in the automotive industry.[23,24] The mono-tube damper is easy to design, but drilling long holes in the piston rod for insertion of wires is difficult. In addition, the output damping force is offset as a result of pressurised gas in the accumulator. The double-ended damper is commonly used in civil engineering;[5,9] it has a piston rod with equal lengths protruding from the ends of the damper housing. It has a simple configuration but needs a large mounting space. The twin-tube MR damper has two fluid reservoirs: one inside the other. The outer reservoir can accommodate the volume change caused by the movement of the piston rod. The twin-tube damper is easier to manufacture than the other configurations. Most commercial passive hydraulic dampers use the twin-tube design. However, due to blockage of MR fluid in the valve, the twin-tube damper is not commonly utilised as an MR damper. In the past decade, several attempts have been made to develop a twin-tube MR damper based on MR fluids.[7,25,26]

In order to realise a practical MR damper for the lateral suspension of a railway vehicle, some design requirements must be taken into account. First, the damper should have a large enough dynamic damping force range to guarantee a fail-safe performance, and the compression and stretch damping forces should be symmetric. Second, the amount of space available to mount the damper is limited; however, despite this point the damper must have a long stroke. Finally, drilling long holes in the position rod should be avoided during the manufacturing process, and the damper must be easy to repair. Thus, the twin-tube style was adopted to design an MR damper for railway vehicles. A bypass MR valve with an electromagnetic circuit outside the hydraulic cylinder was integrated into the damper. The bypass MR valve is easily installed and repaired and exhibits good heat dissipation. A radial flow path of the MR valve was employed since it can generate a higher MR resistance for a given valve length as compared with that for two concentric cylinders in an annular configuration.[27]

A twin-tube MR damper was designed in this project; a schematic diagram of the design is shown in Figure 1. There are two reservoirs in the MR damper: an inner reservoir and an outer reservoir. A bypass MR valve with a radial flow path is connected to the hydraulic cylinder. The inner reservoir is divided into two parts by the piston; a rebound chamber above the piston and a compression chamber below the piston. The piston contains an on-off valve. The inlet passage of the MR valve is connected to the rebound chamber of the inner reservoir, and the outlet passage of the MR valve is connected to the outer reservoir using a connecting tube. A coil is installed in the MR valve to produce a magnetic field. The connecting tube is used to ensure that MR fluid flows continuously between the inner and outer reservoirs no matter where the damper is placed. The outer reservoir is connected to the compression chamber of the inner reservoir through a foot valve. The inner reservoir and MR valve are fully filled with MR fluid, whereas the outer reservoir contains a certain volume of air in addition to MR fluid.

Different on-off valves were designed to make the MR fluid flow in a single direction.

1. When the piston rod is stretched, the piston valve is off, and MR fluid in the rebound chamber is pushed into the MR valve and then into the outer reservoir through the connecting tube. At the same time, there is a vacuum in the compression chamber, and the pressure in outer reservoir is greater than that in the compression chamber. The foot valve that connects the compression chamber and outer reservoir is opened, and MR fluid then flows from the outer reservoir into the compression chamber of the inner reservoir.
2. When the piston rod is compressed, the foot valve is closed, and MR fluid cannot flow between the

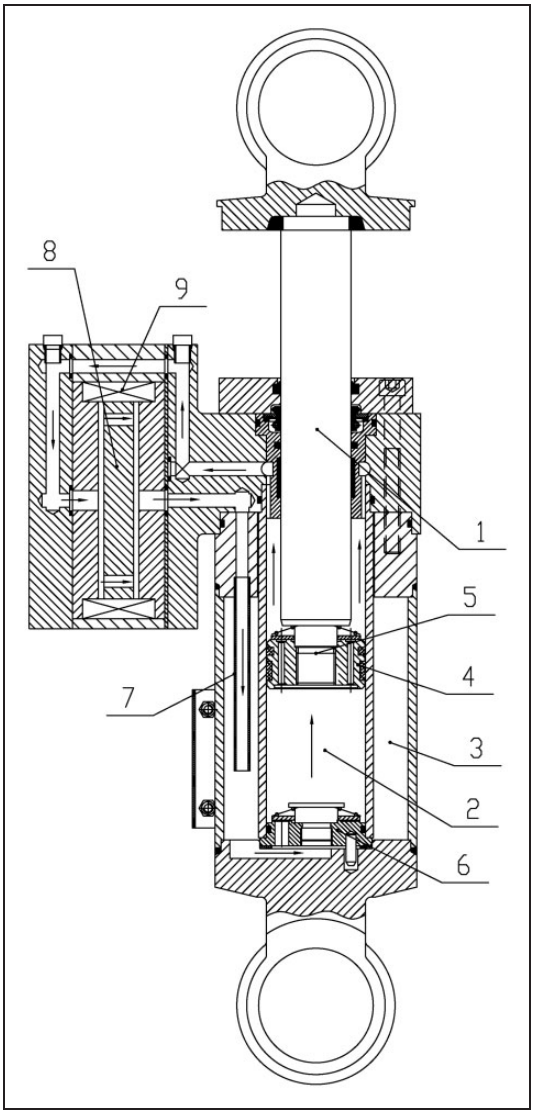

Figure 1. Schematic diagram of the twin-tube and bypass MR damper: (1) piston rod; (2) inner reservoir; (3) outer reservoir; (4) piston valve; (5) piston; (6) foot valve; (7) connecting tube;(8) MR valve; (9) coil.

outer and inner reservoirs. When the piston valve is opened, MR fluid in the inner reservoir flows from the compression chamber to the rebound chamber, then to the MR valve and finally into the outer reservoir. During this process, the outer reservoir accommodates changes in volume caused by the movement of the piston rod.

The single-direction flow (as shown by arrows in Figure 1) can make the compression and stretching force symmetric. In particular, it can make MR fluid flow completely and remix easily in the damper, which improves the anti-sedimentation property of MR fluid in the damper.

Table 1 summarises the parameters of the MR damper based on the installation space available on the suspension of a train. A 114-mm stroke is obtained based on a 170-mm cylinder; this is long enough for the lateral suspension of a railway vehicle. A bypass MR valve with a cuboid shape is installed between the inner and outer reservoirs and occupies a space of $145 \times 130 \times 85$ mm. A coil with 450 turns is embedded in the MR valve. The diameter and height of the MR effect gap are 100 and 0.8 mm, respectively. For this MR damper, a maximum 9-kN force was desired; an appropriate viscous damping force should be generated to make the damper fail-safe if the coil is broken.

Table 1. Parameters of the MR damper.

Stroke	114 mm
Cylinder bore	101 mm
Cylinder length	170 mm
Outer housing diameter	92 mm
Inner housing diameter	50 mm
Piston rod diameter	35.4 mm
MR valve	$145 \times 130 \times 85$ mm
Gap diameter	100 mm
Gap thickness	0.8 mm
Coil	450 turns
Coil resistance	10 Ω

Magnetic analysis of the MR valve

The key part of the MR damper is the MR valve, where the MR effect occurs (part (8) in Figure 1). The output force of the MR damper can be controlled by changing the viscosity of the MR fluid in the MR valve using a coil. Two disks with a radial flow path were designed and placed in the coil. In the lower disk, the MR fluid flows through a central hole and then diffuses between the two parallel plates; in the upper disk, the fluid flows between the two parallel plates and converges into the export orifice. During this process, the flow direction of the MR fluid is always perpendicular to the magnetic field.

For the MR valve, the magnetic circuit is very important, and the as-generated magnetic flux density must be large enough to energise the MR fluid. The finite element software ANSYS 13.0 was used to create a three-dimensional model of the MR valve and analyse the effect of a magnetic field.[28] A sectioned view of the MR valve model is shown in Figure 2; the blue section is MR fluid, the deep sky-blue section is the coil, and the other areas are electrically pure iron (#DT3). The *B–H* curves are given in Figure 3. In post-processing, the two paths AB and CD were created in the MR effect zones, and vertical magnetic field induction was obtained, as shown in Figure 4.

The magnetic flux density in the two paths increases with the applied current, and the maximum value of the magnetic field reaches a value of 0.8 T at a current of 1.75 A. Under the considered current,

the magnetic flux density is uniform except at the points where MR fluids flow in and out of the valve. The magnetic flux densities in the two disks are almost the same at this current. These results indicate that the geometric design is effective and that the electromagnetic circuit can meet the design requirements.

Theoretical analysis

A fluid mechanics-based model is presented that can be used to predict the damping force. The MR fluid was assumed to be an incompressible fluid with steady and laminar flow, and temperature effects were ignored. The main pressure drop of the damper comes from the bypass MR valve. This valve has two main mechanisms to create the drop in viscous pressure:

- fluid flow between the parallel disks;
- fluid flow through the cylindrical passage in the valve.

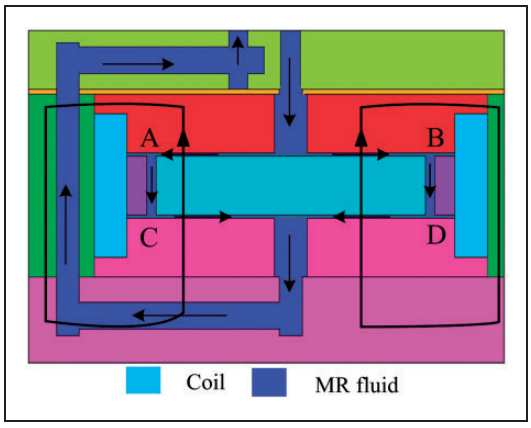

Figure 2. Sectioned view of the MR valve model (arrows show flow of MR fluids and magnetic circuit).

The viscous pressure drop for the MR fluid flowing through parallel disks can be written as[27,29]

$$\nabla P_{\text{vis,dis}} = \frac{6\mu Q}{\pi h^3}\ln\left(\frac{r_2}{r_1}\right) \tag{1}$$

where μ is the zero-field viscosity of the MR fluid, h is the height of the parallel disks, r_2 is the outer radius of the disk, r_1 is the radius of the convergence hole and Q is the volume flow rate through the MR valve. This can be obtained by $Q = \left(A_{\text{pis}} - A_{\text{rod}}\right) V$ at the rebound stroke and $Q = A_{\text{rod}}\, V$ at the compression stroke, where $A_{\text{pis}} = \pi D^2/4$ and $A_{\text{rod}} = \pi d^2/4$ are the areas of the piston and piston rod, respectively, D and d are the diameters of the piston and piston rod, respectively and V is the velocity of the piston.

The viscous pressure drop of the MR fluid flowing through the passage in the valve is

$$\nabla P_{\text{vis,pas}} = \frac{128\mu Q}{\pi D_1^4} L \tag{2}$$

where L is the length of the passage and D_1 is the diameter of the passage.

The pressure drop from the MR effect in a single-stage disk is given as

$$\nabla P_{\text{mr}} = 2.85\frac{\tau_y}{h}(r_2 - r_1) \tag{3}$$

where τ_y is the yield stress of the MR fluid.

Minor pressure losses due to the elbows, expansions, entrance and exit of the damper should be taken into account, especially for high-velocity flows. The overall minor pressure drop can be expressed by

$$\nabla P_{\text{min}} = \frac{K_{\text{L}}\rho\bar{V}^2}{2} \tag{4}$$

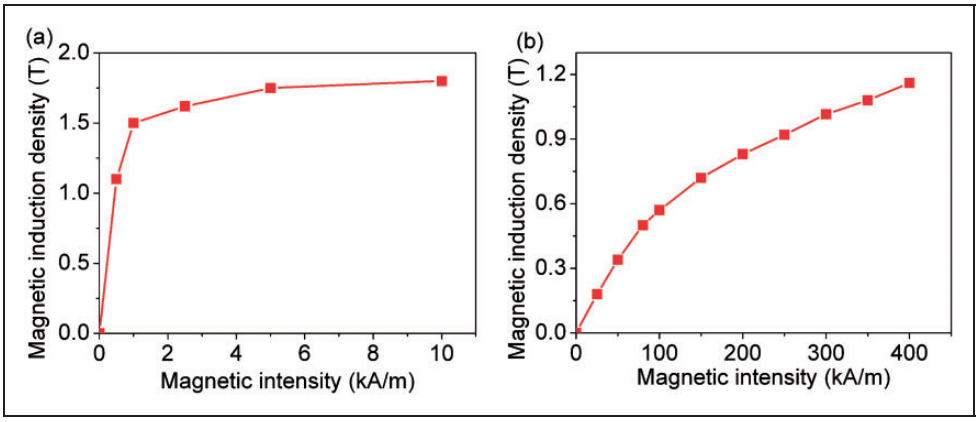

Figure 3. *B–H* curve of (a) MR fluid and (b) electrically pure iron.

where K_L is the minor pressure drop coefficient, ρ is the density of the MR fluid and $\bar{V}^2$ is the average velocity of the MR fluid.

The total pressure drop produced by the MR valve can be given as

$$\nabla P_{MR,val} = 2\nabla P_{mr} + \nabla P_{vis,pas} + 2\nabla P_{vis,dis} + \nabla P_{min} \quad (5)$$

At the rebound stroke (Figure 5), the stretching damping force F_{stre} can be given as

$$F_{stre} = P_{reb}(A_{pis} - A_{rod}) - P_{com}A_{pis} + F_{fric} \quad (6)$$

where P_{reb} and P_{com} are the pressures of the rebound chamber and compression chamber, respectively, and F_{fric} is the friction force acting on the piston and piston rod. From the pressure balance, $\nabla P_{MR,val} = P_{reb} - P_0$ and $\nabla P_{foot} = P_0 - P_{com}$ are obtained, where P_0 is the pressure of the outer reservoir (1 atm) and ∇P_{foot} is the pressure difference of the MR fluid flowing from the outer reservoir to the compression chamber. Here, the volume flow rate can be expressed by $Q_{foot} = A_{pis}V = CA_f\sqrt{2\nabla P_{foot}/\rho}$; thus, $\nabla P_{foot} = (A_{pis}V)^2\rho/2(CA_f)^2$, where A_f is the area of the foot valve and C is the coefficient of discharge. Therefore, equation (6) becomes

$$F_{stre} = (\nabla P_{MR,val} + P_0)(A_{pis} - A_{rod}) - (P_0 - \nabla P_{foot})A_{pis} + F_{fric} \quad (7)$$

Similarly, the damping force of the MR damper at the compression stroke can be obtained by

$$F_{com} = P_{com}A_{pis} - P_{reb}(A_{pis} - A_{rod}) + F_{fric} \quad (8)$$

From the pressure balance, $\nabla P_{MR,val} = P_{reb} - P_0$ and $\nabla P_{piston} = P_{com} - P_{reb}$ are obtained, where ∇P_{piston} is the pressure difference between the compression and rebound chambers. As the volume flow rate is a $Q_{piston} = A_{pis}V = CA_p\sqrt{2\nabla P_{piston}/\rho}$, $\nabla P_{piston} = (A_{pis}V)^2\rho/2(CA_p)^2$, where A_p is the area of the piston valve. Accordingly, equation (8) becomes

$$F_{com} = \nabla P_{piston}A_{pis} + (\nabla P_{MR,val} + P_0)A_{rod} + F_{fric} \quad (9)$$

Because of the symmetry of the damping force at the rebound and compression strokes, $F_{stre} = F_{com}$; thus

$$(\nabla P_{MR,val} + P_0)(A_{pis} - A_{rod}) - (P_0 - \nabla P_{foot})A_{pis} + F_{fric} = \nabla P_{piston}A_{pis} + (\nabla P_{MR,val} + P_0)A_{rod} + F_{fric} \quad (10)$$

As ∇P_{foot}, ∇P_{piston} and P_0 are far less than $\nabla P_{MR,val}$, equation (10) becomes

$$(\nabla P_{MR,val} + P_0)(A_{pis} - A_{rod}) = (\nabla P_{MR,val} + P_0)A_{rod} \quad (11)$$

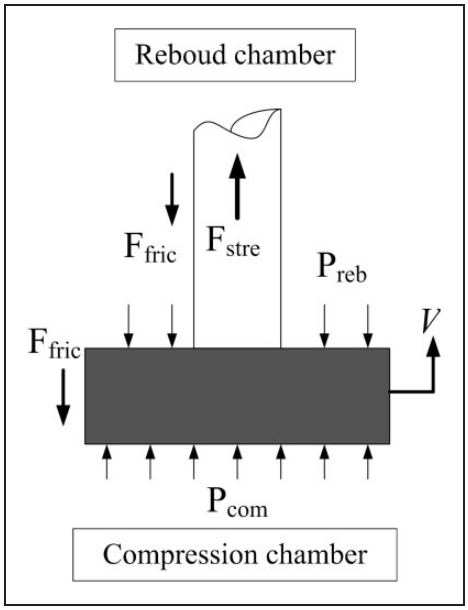

Figure 5. Free-body diagram of piston.

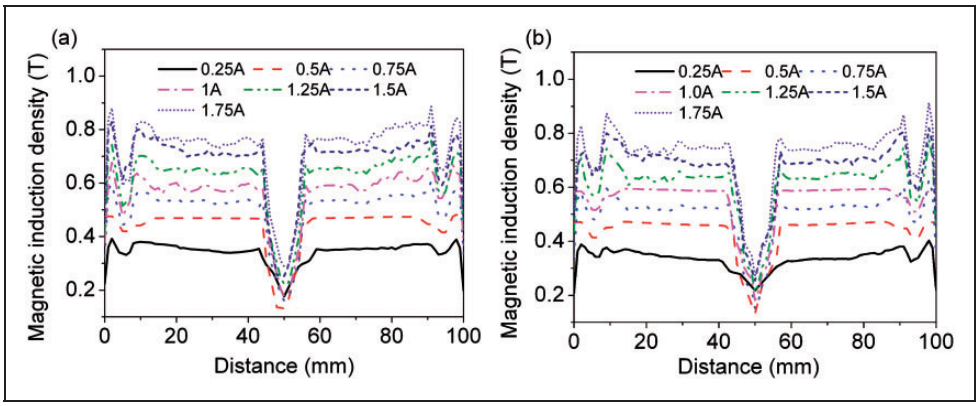

Figure 4. Distribution of magnetic flux density at (a) the CD path and (b) the AB path for different applied currents.

Thus, $A_{pis} = 2A_{rod}$; that is, $D = \sqrt{2}d$.
Finally, the damping force can be simplified to

$$F_{stre} = F_{com} = \nabla P_{MR,val} A_{rod} + F_{fric} + F_{val} \quad (12)$$

where F_{val} is the damping force generated by the foot valve or piston valve.

Experiment results

MR fluid

MR fluid with a 30% volume fraction was prepared by mixing carbonyl iron powder particles (CN, BASF, Germany; average particle size of about 6 μm) in silicone oil (H201, Sinopharm Chemical Reagent Co. Ltd., China; viscosity of about 20 mPa·s). Then, stearic acid (2 wt %) was added to improve its anti-sedimentation property. After 1 day, clear separation between the iron particles and the oil was observed, but the iron particles and the oil were easily remixed by shaking the mixture.

The rheological behaviour of the MR fluid was measured by a parallel-plate magnetorheometer (Physica MCR 301, Anton Paar, Austria). Figure 6 shows the shear stress of the MR fluid against shear rate at various magnetic fields. The shear stress increases with the applied magnetic field. Shear thinning occurs when the level of shear was increased in a given field. The yield stress was obtained by the extrapolating shear stress data back to the zero shear level based on Bingham's model. Polynomial fitting was used to capture the relation between the yield stress and magnetic field: τ_y (kPa) $= 111.08B^4 - 241.38B^3 + 140.69B^2 + 17.133B + 0.0316$. Figure 7 The zero field viscosity of the MR fluid is about 0.7 Pa·s, and the saturated yield stress is about 28 kPa.

MR damper

A practical twin-tube- and bypass-containing MR fluid damper was fabricated and tested with the MTS system (Figure 8). A DC power supply (CA-YD, Sinocera Piezotronics Inc., China) was utilised to energise the coil. The displacement control mode was used to create the sinusoidal excitation, and the damping force and displacement with time were obtained using a force sensor and LVDT. The testing was conducted at a constant temperature of 25°C, and the velocity was acquired from the displacement differential with time.

As shown in Figure 9, typical force–displacement and force–velocity plots were obtained under various currents. A 15-mm amplitude and 1-Hz frequency sinusoidal excitation were used in the harmonic excitation test. The damping forces clearly increase with the current. When the current is not applied, the damping forces for the rebound and compression stroke are almost 1 kN; this represents the minimum damping force. When 1.6 A is applied, the damping force reaches 9 kN. Therefore, the dynamic coefficient of control force has a value of nine. The zero-field force can ensure that the MR damper is a fail-safe device, and the geometry of the valve can be designed to obtain the expected damping force. Similar results were also obtained when the amplitude and frequency of the sinusoidal excitation were 25 mm and 1 Hz, respectively (Figure 10). When the current is 0 A, the damping force is larger for the 25-mm amplitude case than for the 15-mm amplitude case. The shear rate is larger for the 25-mm amplitude case than for the 15-mm amplitude case; for a Newtonian fluid the damping force is larger at a large velocity than at a small velocity. However, after the current was applied, the damping force is smaller for the 25-mm amplitude case than for the 15-mm amplitude case, which may be a result of shear thinning of the MR fluid. When the extent of shear increases, the shear

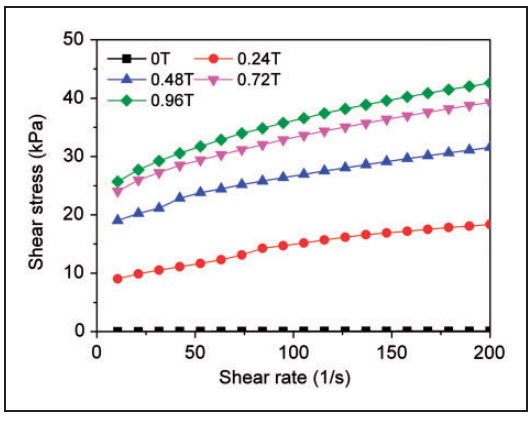

Figure 6. Shear stress of MR fluid versus shear rate for various values of the magnetic field.

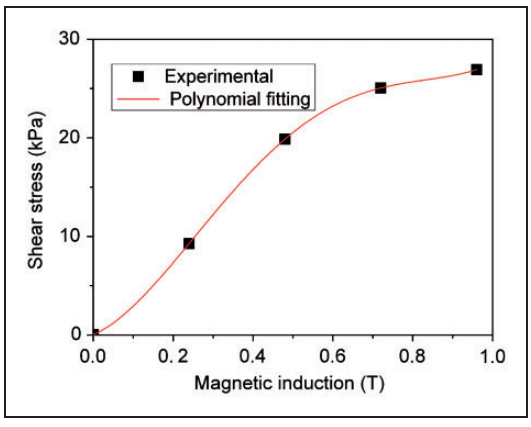

Figure 7. Polynomial fitting for shear yield stress with magnetic induction.

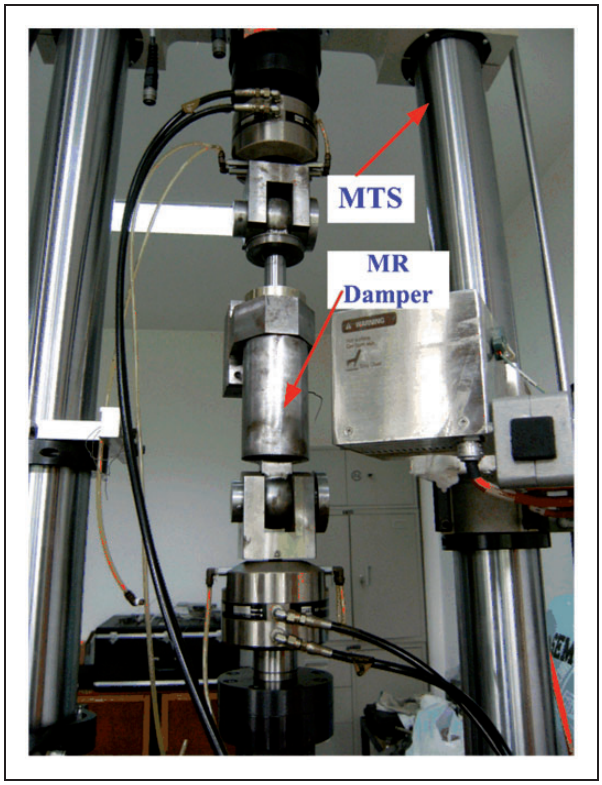

Figure 8. MR damper and test setup.

stress of the MR fluid decreases; thus, the damping force of MR damper decreases.

The symmetry of the damping force is an important aspect for assessing the MR damper, and the level of asymmetry of the force $\varepsilon = |(F_{stre} - F_{com})/(F_{stre} + F_{com})| \times 100\%$ can be used to evaluate the damper. The extent of asymmetry in the damping force as a function of the applied current was obtained at amplitudes of the sinusoidal excitation of 15 and 25 mm (Figure 11). Asymmetric damping forces are found to occur as a result of the pressure difference between the rebound and compression strokes. The volume flow rate differences for the rebound and compression strokes lead to the difference in viscous pressure. The extent of asymmetry decreases with an increase in the applied current, and the maximum value occurs at 0 A. The level of asymmetry is about 4% and 3% at the 15- and 25-mm amplitudes, respectively. After the current is applied, the level of asymmetry changes to about 1%. Increasing the applied current increases the damping force generated by the MR effect. The damping force generated by the MR effect is the same at the rebound and compression strokes. Therefore, the extent of asymmetry in the force becomes smaller as the current increases. The foot and piston valves can also be

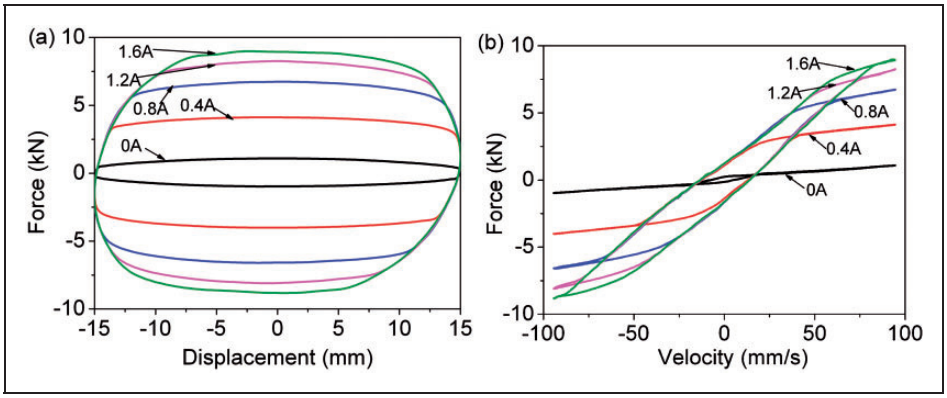

Figure 9. (a) Force–displacement and (b) force–velocity relationships of MR damper.

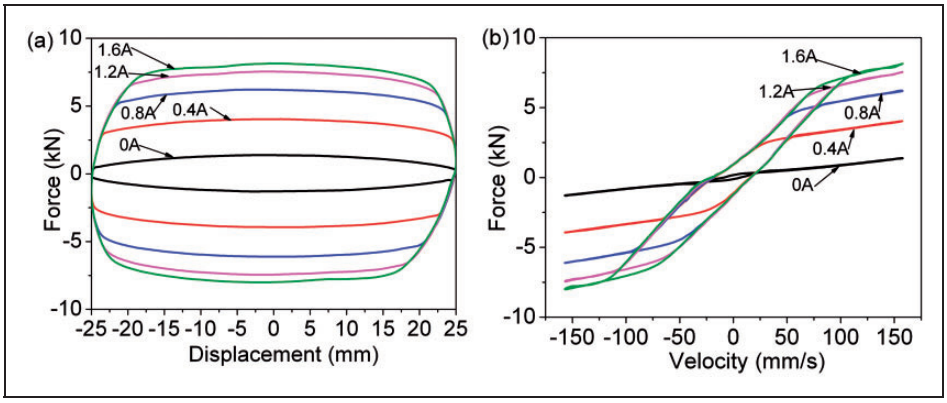

Figure 10. (a) Force–displacement and (b) and force–velocity relationships of MR damper.

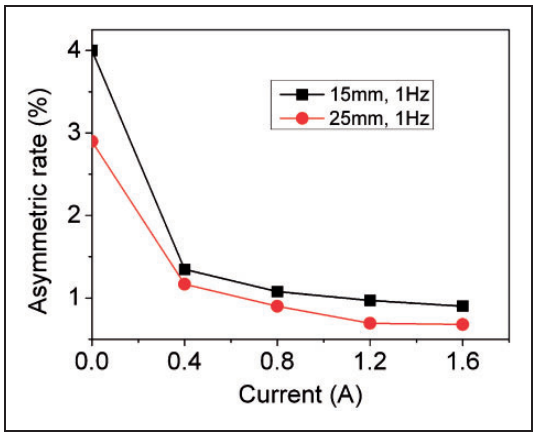

Figure 11. Level of asymmetry in the damping force created by the MR damper.

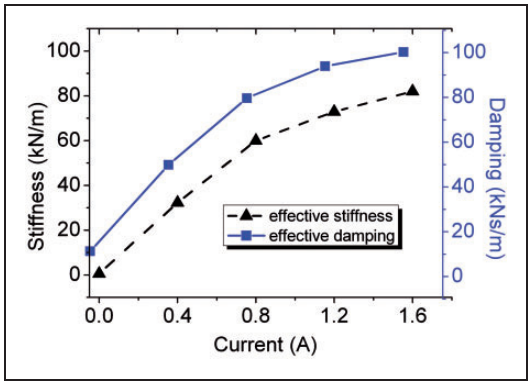

Figure 12. Equivalent stiffness and damping of MR damper.

improved to compensate for the viscous pressure difference in the MR valve and obtain a more symmetric force.

An equivalent linear model,[30] which considers the effective elastic stiffness and effective viscous damping, was used to predict the force developed in the MR damper

$$F_{\mathrm{MRD}} = k_{\mathrm{eff}} x + c_{\mathrm{eff}} \dot{x} \tag{13}$$

where F_{MRD} is the resultant force provided by the MR damper, k_{eff} is the effective stiffness, c_{eff} is the effective viscous damping constant and x and $\dot{x}$ are the base displacement and velocity, respectively. The two parameters k_{eff} and c_{eff} were determined by studying the experimental force–displacement hysteresis loops. k_{eff} is the slope of the peak-to-peak values of the hysteresis loop and c_{eff} can be calculated using the following equation

$$c_{\mathrm{eff}} = \frac{E_{\mathrm{loop}}}{\pi \omega A^2} \tag{14}$$

where E_{loop} is the energy dissipation per cycle of loading, A is the displacement amplitude and ω is the frequency.

Figure 12 shows the identified field-dependent equivalent stiffness and damping. They both increase with an increase in the current. The stiffness of the MR damper is about 100 times larger at 1.6 A than at zero field, and the effective damping factor is about nine times larger. At 0 A, the damper behaves as a viscous damper with a stiffness of almost zero. When a current is applied, the MR damper acts like a viscous damper and spring combination system; this is because the MR fluid in the damper behaves as a viscoelastic material under a magnetic field.

The response time of the MR fluid was also measured. A triangular excitation with a 15-mm amplitude and a 0.5-Hz frequency was applied to the MR damper. The current was changed directly between 0 and 1 A. As shown in Figure 13, the damping force changes from 300 to 5440 N after the current abruptly changes from 0 to 1 A (Figure 13(a)) and changes from 5790 to 1200 N after the abruptly changes from 1 to 0 A (Figure 13(b)). A recent report has stated that the force cannot return to the initial value (300 N) when the current is removed as a result of residual magnetism.[31] The response time of the MR damper is defined as the time needed to achieve a 90% change in force. Under this definition the increasing response time is 0.342 s and the decreasing response time is 0.29 s. The response time is associated with the applied amplitude, frequency, changing current, etc.,[32] but the change is small. The response time of the MR damper is large in the present study; this is mainly due to the compressibility of the MR fluid in the rebound or compression stroke.[33] As shown in Figures 9 and 10, the compressibility of the MR fluid causes the force–displacement loops to be slightly oblique. Thus, the time delay has to be compensated in actual semi-active control.[34]

Sedimentation of the MR damper was investigated. First, the damper was tested with a sinusoidal excitation of 15-mm amplitude and 1-Hz frequency at different currents. After 6 days, the damper was again excited under the same condition for a further 100 cycles without current being applied. The results showed that the damping force was reduced after 6 days. Increasing the current greatly decreased the force; the decrease in the force levels reached as high as 1 kN. The anti-sedimentation of MR fluid was clearly poor in the present work. However, the MR damper quickly recovered after a short excitation even after standing for a long time; this must be due to the single flow direction of the MR fluid in the damper. The foot and piston valves were designed as on–off valves, and the areas of the valve were sufficiently large. Therefore, aggregation of MR fluid in the valve is difficult to produce, and the sedimentation of the twin-tube MR damper was tiny for a system intended for use on a railway vehicle.

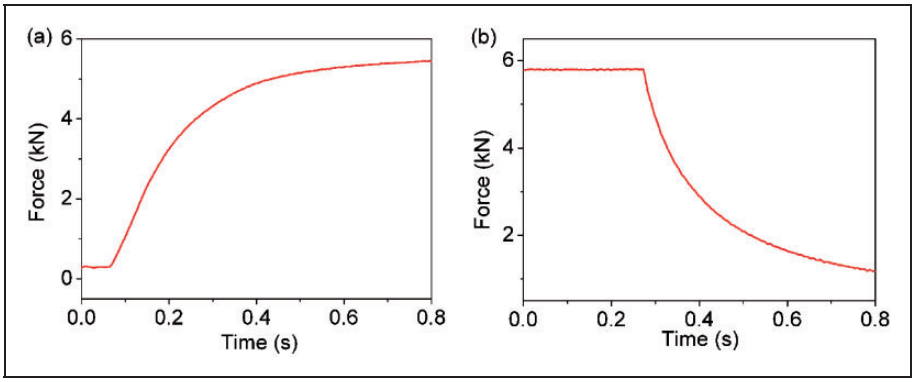

Figure 13. Evolution of the damping force as a function of time as the current is changed: (a) increasing from 0 to 1 A and (b) decreasing from 1 to 0 A.

Conclusions

In this study, a practical twin-tube- and bypass-containing damper for railway vehicles was designed, fabricated and tested. This MR damper exhibited a maximum damping force of 9 kN and a dynamic coefficient of nine. Sufficient damping force at a 0-A current was achieved to ensure the damper is a fail-safe device. The advantages of the designed damper are its large stroke and ease of manufacture. A radial flow path was embedded into the bypass valve to save installation space. The unique unidirectional flow path prevents sedimentation in the MR damper.

A three-dimensional finite element analysis was conducted to evaluate the magnetic field strength inside MR fluid. This analysis indicated that the area of the piston rod must be half that of the piston, which makes the damping force symmetric during the rebound and compression strokes. The extent of asymmetry in the force created by the damper was found to be less than 4% at various currents. The response time of the MR damper was found to be about 0.3 s, which was mainly derived from the compressibility of MR fluid. Future work will involve testing the MR damper on railway vehicles.

Funding

This work was financially supported by the National Natural Science Foundation of China (grants 11125210, 11072234, 11102202), the National Basic Research Programme of China (2012CB937500) and The Chinese Academy of Sciences for Key Topics in Innovation Engineering (grant KJCX2-EW-L02).

Acknowledgements

We wish to thank Xianhu Xiang, Jianfeng Li and Qun Xue for their insightful discussions. We also thank the staff of the Zhuzhou Electric Locomotive Research Institute for their support during the creation of the MR damper.

References

1. De Vicente J, Klingenberg DJ and Hidalgo-Alvarez R. Magnetorheological fluids: a review. *Soft Matter* 2011; 7: 3701–3710.
2. Carlson JD, Catanzarite DM and Clair KA. Commercial magnetorheological fluid devices. *Int J Mod Phys B* 1996; 10: 2857–2865.
3. Gudmundsson K, Jonsdottir F and Thorsteinsson F. A geometrical optimization of a magneto-rheological rotary brake in a prosthetic knee. *Smart Mater Struct* 2010; 19: 035023.
4. Dyke SJ, Spencer BF, Sain MK and Carlson JD. An experimental study of MR dampers for seismic protection. *Smart Mater Struct* 1998; 7: 693–703.
5. Yang G, Spencer BF, Carlson JD and Sain MK. Large-scale MR fluid dampers: modeling and dynamic performance considerations. *Engng Struct* 2002; 24: 309–323.
6. Jacobs SD, Arrasmith SA, Kozhinova IA, et al. An overview of magnetorheological finishing (MRF) for precision optics manufacturing. *Ceram Trans* 1999; 102: 185–199.
7. Simon D and Ahmadian M. Vehicle evaluation of the performance of magnetorheological dampers for heavy truck suspensions. *J Vib Acoust* 2001; 123: 365–375.
8. Lindler JE, Choi YT and Wereley NM. Double adjustable shock absorbers utilizing electrorheological and magnetorheological fluids. *Int J Veh Des* 2003; 33: 189–206.
9. Tu JW, Liu J, Qu WL, et al. Design and fabrication of 500-kN large-scale MR damper. *J Intell Mater Syst Struct* 2011; 22: 475–487.
10. O'Neill HR and Wale GD. Semi-active suspension improves rail vehicle ride. *Comput Control Engng J* 1994; 5: 183–188.
11. Lau YK and Liao WH. Design and analysis of magnetorheological damper for train suspension. *Proc IMechE, Part F: J Rail Rapid Transit* 2005; 219: 261–276.
12. Liao WH and Wang DH. Semi active vibration control of train suspension systems via magnetorheological dampers. *J Intell Mater Syst Struct* 2003; 14: 161–172.
13. Wang DH and Liao WH. Semi-active suspension systems for railway vehicles using magnetorheological

dampers, part I: system integration and modeling. *Veh Syst Dyn* 2009; 47: 1305–1325.
14. Wang DH and Liao WH. Semi-active suspension systems for railway vehicles using magnetorheological dampers, part II: simulation and analysis. *Veh Syst Dyn* 2009; 47: 1439–1471.
15. Atray VS and Roschke PN. Design, fabrication, testing, and fuzzy modeling of a large magnetorheological damper for vibration control in a railcar. In: DP Burleson and DL Cackovic (eds) *The IEEE/ASME joint rail conference*, Chicago, Illinois, 22–24 April 2003, pp. 223–229. Piscataway, NJ: IEEE.
16. Atray VS and Roschke PN. Neuro-fuzzy control of vertical vibrations in a railcar using magnetorheological dampers. *Comput-Aided Civil Infrastruct Eng* 2004; 19: 81–92.
17. Pugi L, Bartolini, F, Rinchi M and Meli E. Design of a lateral and vertical semi-active suspension system for a high speed train. In: J Fraczek (ed.) *The multibody dynamic eccomas thematic conference*, Warsaw, Poland, 29 June–2 July 2009.
18. Pugi L, Rindi A, Bartolini F and Auciello J. Simulation of a semi-active suspension system for a high speed train. In: M Berg and AS Trigell (eds) *The 21st IAVSD symposium on dynamics of vehicles on roads and tracks*, Stockolm, Sweden, 17–21 August 2009.
19. Allotta B, Pugi L, Bartolini F, et al. Comparison of different control approaches aiming at enhancing the comfort of a railway vehicle. In: B Yao (ed.) *The IEEE/ASME international conference on advanced intelligent mechatronics*, Montréal, Canada, 6–9 July 2010, pp. 676–681. Piscataway, NJ: IEEE.
20. Gao GS and Yang SP. Semi-active control performance of railway vehicle suspension featuring magnetorheological dampers. In: FH Luo (ed.) *The first IEEE conference on industrial electronics and applications*, Singapore, 24–26 May 2006, pp. 1–5. Piscataway, NJ: IEEE Press.
21. Hudha K, Harun MH, Harun MH and Jamaluddin H. Lateral suspension control of railway vehicle using semi-active magnetorheological damper. In: C Stiller (ed.) *The IEEE intelligent vehicles symposium*, Baden-Baden, Germany, 5–9 June 2011, pp. 728–733. Piscataway, NJ: IEEE Press.
22. Poynor JC. *Innovative design for magneto-rheological dampers*. MS Thesis, Virginia Polytechnic Institute and State University, USA, 2001.
23. Choi SB, Nam MH and Lee BK. Vibration control of a MR seat damper for commercial vehicles. *J Intell Mater Syst Struct* 2000; 11: 936–944.
24. Li WH, Yao GZ, Chen G, et al. Testing and steady state modeling of a linear MR damper under sinusoidal loading. *Smart Mater Struct* 2000; 9: 95–102.
25. Zhou GY and Zhang PQ. Investigation of the dynamic mechanical behavior of the double-barreled configuration in a magnetorheological fluid damper. *Smart Mater Struct* 2002; 11: 230–238.
26. Sassi S, Cherif K, Mezghani L, et al. An innovative magnetorheological damper for automotive suspension: from design to experimental characterization. *Smart Mater Struct* 2005; 14: 811–822.
27. Wang X, Gordaninejad F, Hitchcock G, et al. A new modular magnetorheological fluid valve for large-scale seismic applications. *Proc SPIE* 2004; 5386: 226–237.
28. Li WH, Du H and Guo NQ. Finite element analysis and simulation evaluation of a magnetorheological valve. *Int J Adv Mfg Technol* 2003; 21: 438–445.
29. Aydar G, Wang X and Gordaninejad F. A novel two-way-controllable magneto-rheological fluid damper. *Smart Mater Struct* 2010; 19: 065024.
30. Li WH, Zhang XZ and Du H. Development and simulation evaluation of a magnetorheological elastomer isolator for seat vibration control. *J Intell Mater Syst Struct* 2012; 23: 1041–1048.
31. Gorodkin S, James R and Kordonski W. Irreversible effects in magnetorheological fluids. *J Intell Mater Syst Struct* 2011; 22: 1749–1754.
32. Koo JH, Goncalves FD and Ahmadian M. A comprehensive analysis of the response time of MR dampers. *Smart Mater Struct* 2006; 15: 351–358.
33. Guan XC and Ou JP. Response time experiment and analysis of magnetorheological fluid actuator. *Earthq Engng Engng Vib* 2002; 22: 96–102 (in Chinese).
34. Xu ZD, Shen YP and Guo YQ. Semi-active control of structures incorporated with magnetorheological dampers using neural networks. *Smart Mater Struct* 2003; 12: 80–87.